Sensors and Actuators B 248 (2017) 9–18

Contents lists available at ScienceDirect

Sensors and Actuators B: Chemical

journal homepage: www.elsevier.com/locate/snb

# Highly sensitive gas sensor based on stabilized zirconia and $CdMoO_4$ sensing electrode for detection of acetone

Fangmeng Liu[b], Ce Ma[b], Xidong Hao[b], Chunhua Yang[c], Hongqiu Zhu[c], Xishuang Liang[a,b,*], Peng Sun[b], Fengmin Liu[b], Xiaohong Chuai[b], Geyu Lu[a,b,*]

[a] State Key Laboratory of Automotive Simulation and Control, Jilin University, 5988 Renmin Avenue, Changchun 130012, China
[b] State Key Laboratory on Integrated Optoelectronics, College of Electronic Science and Engineering, Jilin University, 2699 Qianjin Street, Changchun 130012, China
[c] School of Information Science and Engineering, Central South University, Changsha 410083, China

ARTICLE INFO

*Article history:*
Received 27 December 2016
Received in revised form 25 February 2017
Accepted 27 March 2017
Available online 29 March 2017

*Keywords:*
Acetone sensor
$CdMoO_4$
YSZ
Mixed potential

ABSTRACT

A highly sensitive mixed potential type gas sensor based on stabilized zirconia (YSZ) and $CdMoO_4$ sensing electrode (SE) was developed and used for detection of acetone at 625 °C. By comparing the sensing performance for different devices fabricated, the sensor utilizing $CdMoO_4$-SE exhibited the highest response value (−133.5 mV) to 100 ppm acetone at 625 °C, and even could achieve low detection limit of 500 ppb at 625 °C. The sensor attached with $CdMoO_4$-SE displayed high sensitivity of −84 mV/decade to acetone in the range of 5–300 ppm at 625 °C. The present device also showed good repeatability, selectivity to certain deleterious gases, moisture resistance and acceptable drifts in 10 days measured period at 625 °C, demonstrating great potential for practical application in acetone sensing detection. Additionally, the sensor involving mixed potential mechanism was proposed and further clarified by polarization curve.


## 1. Introduction

Air pollution associated with photochemical smog and haze-fog, characterized by high levels of ozone ($O_3$) and fine particulates (PM2.5), has emerged as one of the most severe environmental pollution issues owing to the process of accelerated urbanization and industrialization in China [1,2]. As key precursors of $O_3$ and PM2.5, volatile organic compounds (VOCs) are composed of hundreds of species, which are directly emitted into the atmosphere from a variety of natural and anthropogenic sources. The major anthropogenic emission sources of VOCs include vehicular exhaust, fuel evaporation, industrial processes, household products and solvent usage, etc. [3–5]. Among different of species, acetone as a kind of important material of VOC, not only cause serious environmental damage but also cause a loose to human body when long-term inhalation or contact. Although some expensive and cumbersome analysis detection technology has been widely used [6–8], but the new effective method and strategy characterized with cost-effective, portable and real-time detection are still expected. The miniaturized and robust mixed potential type solid-state electrochemical gas sensing device based on yttria-stabilized zirconia (YSZ) electrolyte has great potential in aspect of monitoring acetone owing to good stability as well as high sensitivity and selectivity.

So far, the mixed potential type gas sensor based on YSZ and metal oxides sensing electrode has been extensively investigated and developed to detect different kinds of poisonous and detrimental gases, such as $NO_x$ [9–11], $NH_3$ [12–14], CO [15,16], $H_2S$ [17] and VOCs [18–20]. Additionally, our group developed successively two kinds of YSZ-based mixed potential type gas sensor utilzing $Zn_3V_2O_8$-SE [21] and $NiNb_2O_6$-SE [22] to monitor acetone. The sensor attached with $Zn_3V_2O_8$-SE exhibited response value of −69 mV to 100 ppm acetone and sensitivity of −56 mV/decade to acetone concentration in the range of 10–400 ppm at 600 °C. The sensor using $NiNb_2O_6$-SE showed the sensitivity of −79 mV/decade to acetone in the concentration range of 5–500 ppm and the response value of the sensor to 100 ppm acetone was approximately −113 mV at 650 °C. Based on previous research result, some excellent works have been done. Nevertheless, further development of acetone sensor with higher sensitivity still faces great challenges in the process of practical application. According to mixed potential type model, however, the enhanced sensitivity was depended on the electrochemical catalytic activity of sensing electrode material to target gas at TPB. Therefore, investigation on new

* Corresponding authors at: State Key Laboratory on Integrated Optoelectronics, College of Electronic Science and Engineering, Jilin University, 2699 Qianjin Street, Changchun 130012, China.
*E-mail addresses:* liangxs@jlu.edu.cn (X. Liang), lugy@jlu.edu.cn (G. Lu).

http://dx.doi.org/10.1016/j.snb.2017.03.133
0925-4005/

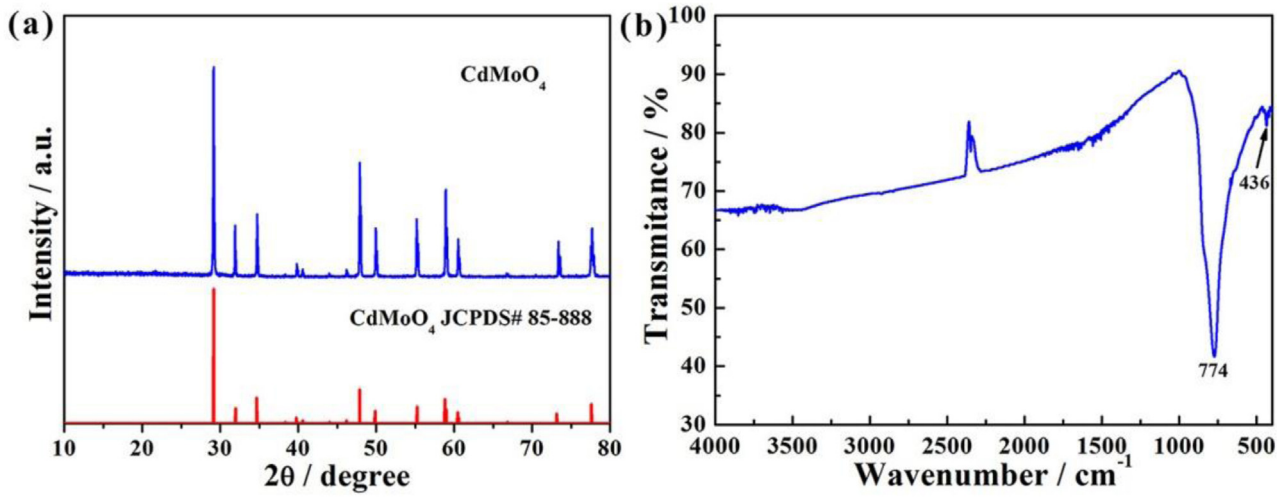


**Fig. 1.** (a) XRD pattern and (b) FT-IR spectrum of $CdMoO_4$ composite oxide material.

type sensing electrode material is an effective way to achieve highly sensitive acetone sensor.

In this work, three kinds of mixed potential type stabilized zirconia (YSZ)-based acetone sensors using new type sensing electrodes ($CdMoO_4$, $CoMoO_4$ and $NiMoO_4$) were developed successfully, aiming at fast and available detection of acetone in the atmosphere environment. For three sensing devices fabricated, the sensor attached with $CdMoO_4$-SE achieved the highest response value to 100 ppm acetone at 625 °C. Moreover, the corresponding sensing characteristics for the present sensor, such as sensitivity, selectivity, repeatability, moisture resisitance and stability, were studied in detail and sensing mechanism involving mixed potential was discussed.

## 2. Experimental

### 2.1. Preparation and characterization of $CdMoO_4$ sensing electrode material

Cadmium nitrate tetrahydrate ($Cd(NO_3)_2{\cdot}4H_2O$) and Sodium Molybdat Dihydrat ($Na_2MoO_4{\cdot}2H_2O$) were purchased from Sinopharm Chemical Reagent Co., Ltd. $CdMoO_4$ nanoparticles were synthesized via a facile magnetic stirring method. Typically, 3 mmol $Na_2MoO_4{\cdot}2H_2O$ was dissolved in 20 mL of deionized water under magnetic stirring vigorously. Then, 10 mL of aqueous solution containing 3 mmol $Cd(NO_3)_2{\cdot}4H_2O$ was dropwise added into above solution and stirring for 3 h. The precipitate was collected via centrifugation and washed with deionized water and absolute ethanol several times, and dried at vacuum drying oven of 80 °C. Finally, the target product was sintered at 800 °C for 2 h using a muffle furnace. $MMoO_4$ (M: Ni, and Co) sensing materials were obtained with the same method according to above-described procedure, respectively.

The structural properties of the products were characterized with Rigaku wide- angle X-ray diffractometer (D/max rA, using Cu Kα radiation at wave length = 0.1541 nm) in the angular range of 10–80°. Fourier transform infrared spectroscopy (FTIR) of the $CdMoO_4$ sensing electrode material was recorded in the wavenumber range of 4000–400 $cm^{-1}$ with a PE-400 spectrometer at room temperature. A technique of power pellets with KBr at a mass ratio of 1:200 was applied. Field-emission scanning electron microscopy (FESEM) measurements of surface morphology of the $CdMoO_4$-SE materials were performed using a JEOL JSM-7500F microscope with an accelerating voltage of 15 kV. X-ray photoelectron spectroscopy (XPS) measurements were performed on a Thermo ESCALAB250 spectrometer equipped with an Al-Kα ray source.

### 2.2. Fabrication and measurement of gas sensor

The sensor was fabricated using the YSZ plate (8 mol% $Y_2O_3$-doped, 2 mm × 2 mm square, 0.2 mm thickness, provided by Tosoh Corp., Japan). A point-shaped and a narrow stripe-shaped Pt electrode (reference electrode, RE) were formed on two ends of the YSZ plate using a commercial Pt paste (Sino-platinum Metals Co., Ltd.). The various sensing electrode materials ($CdMoO_4$, $CoMoO_4$ and $NiMoO_4$) were mixed with a minimum quantity of deionized water, respectively. Then, the resultant paste was applied on the point-shaped Pt to form stripe-shaped sensing electrode (SE), and then the device was sintered at 800 °C for 2 h to gain good contact between the sensing electrode and electrolyte. The Pt heater printed on $Al_2O_3$ substrate was then fixed to the YSZ plate by the inorganic adhesive, which provided the required heating temperature for the sensor. The schematic of the fabricated sensor as shown in our previous papers [21,22], the YSZ as the electrolyte and the $MMoO_4$ (M:Cd, Ni and Co) and Pt are sensing electrode and reference electrode, respectively.

The gas sensing characteristics of the fabricated sensors were measured by a conventional static method. The detailed gas sensing measurement process was performed according to our previous work [23,24]. The electric potential difference (V) between the SE and the RE was measured with a digital electrometer (Rigol Technologies, Inc., DM3054, China) when the sensor was exposed to air or sample gas. The results obtained were recorded with a computer connected to the electrometer. The same times exposed to air and different concentrations of sample gases are kept consistent in each measurement concentration situation and the response signal exposed to sample gas at last minute as the calibration of potential value to assure the accuracy. The current–voltage (polarization) curves of the sensor were carried out via the potentiodynamic method (CHI650C, Instrument corporation of Shanghai, China) using a two-electrode configuration in the base gas (air) and the different concentrations of acetone gas (20, 50 and 100 ppm) at 625 °C. The sensing electrode connector of CHI600C Instrument linked with sensing electrode of the sensor, and the reference and counter electrodes simultaneously connected to the same reference electrode of the sensor. The complex impedance measurements of the sensors in air and 100 ppm of various deleterious gases were performed by using an impedance analyzer (Solartron, 1260 and

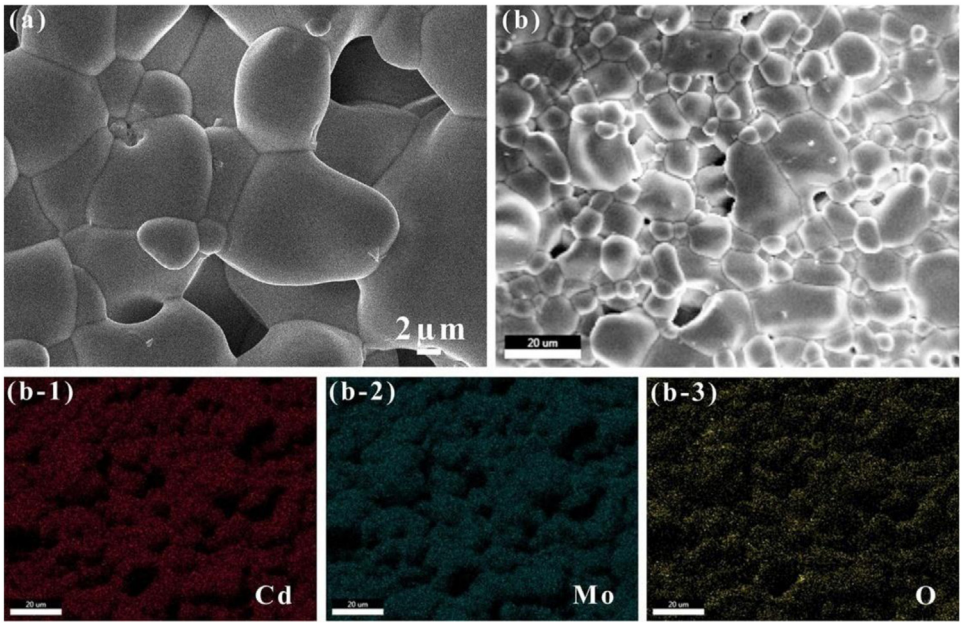


**Fig. 2.** SEM images of $CdMoO_4$-SE material; (b) EDS mapping images for the element of Cd, Mo and O of $CdMoO_4$.

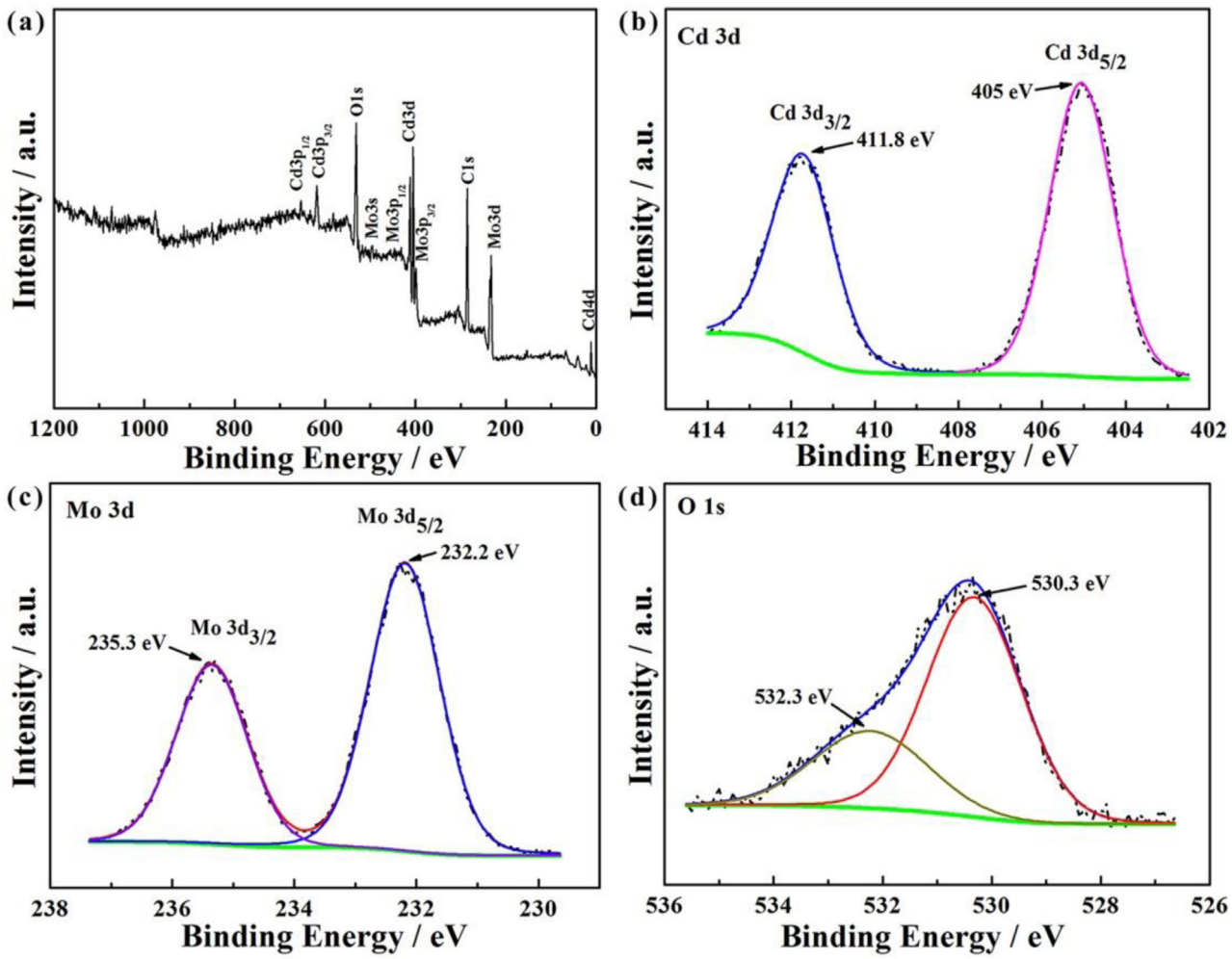


**Fig. 3.** XPS spectra of $CdMoO_4$ composite oxide material (a) survey, (b) Cd 3d, (c) Mo 3d, (d) O 1s.

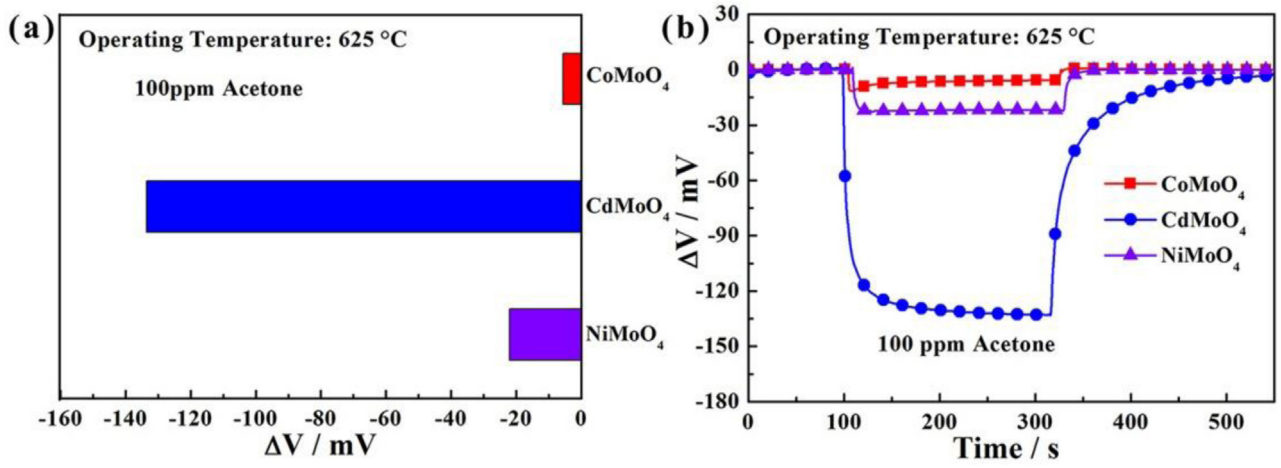


**Fig. 4.** Response of sensors attached with different sensing electrode materials to 100 ppm acetone at 625 °C.

**Table 1**
Comparison of the mixed potential estimated and the potential difference value observed for the fabricated sensors to acetone at 625 °C.

| Sensors | Acetone Conc. (ppm) | Mixed potential (estimated) (mV) | Potential difference value (observed) (mV) |
|---|---|---|---|
| $NiMoO_4$-SE | 100 | −24 | −22 |
| $CoMoO_4$-SE | 100 | −6.5 | −5.5 |
| $CdMoO_4$-SE | 100 | −134 | −133.5 |
| $CdMoO_4$-SE | 20 | −77 | −76.5 |
| $CdMoO_4$-SE | 50 | −106 | −105 |

**Table 2**
Comparison of the sensing performance of the present sensor and those of devices reported in literatures.

| Material | Acetone Conc. (ppm) | Response (mV) | Sensitivity (mV/decade) | Low Detection limit (ppm) | Reference |
|---|---|---|---|---|---|
| $CdMoO_4$ | 100 | −133.5 | −84 | 0.5 | Present work |
| $NiNb_2O_6$ | 100 | −113 | −79 | 0.5 | [22] |
| $Zn_3V_2O_8$ | 100 | −69 | −56 | 1 | [21] |
| $NiCr_2O_4$ | 100 | −60 | −22 | – | [42] |
| $SnO_2$ | 100 | 22 | 45 | – | [43] |
| $Pt/CeO_2/SnO_2$ | 100 | 19 | 36 | – | [43] |

Solartron, 1287) in the frequency range of 0.1 Hz–1 MHz at 625 °C. The amplitude of the AC potential signal was fixed at 300 mV in all measurements.

## 3. Results and discussion

X–ray diffraction (XRD) was used to identify the crystallographic structure and crystallinity of the as-synthesized products. Fig. 1(a) shows the XRD pattern of $CdMoO_4$ composite oxide material. The sharp diffraction features suggested the good crystalline nature of the prepared $CdMoO_4$ composite oxide sensing electrode material. The diffraction peaks of $CdMoO_4$ are readily indexed to tetragonal structure of $CdMoO_4$ oxide standard XRD patterns, which agreed well with the reported values from JCPDS#85-888. No impurity phases were observed from the pattern, which suggests the high purity of material. Additionally, FT-IR spectrum of $CdNb_2O_6$ sensing electrode material was performed and results obtained is shown in Fig. 1(b). The absorption peak at 774 $cm^{-1}$ in the range of 740–890 $cm^{-1}$ can be assigned to the stretching vibration of O-Mo-O in $[MoO_4]^{2-}$ tetrahedrons and the Mo-O weak bending vibration appears at 436 $cm^{-1}$. These results are in accordance with those previously reported [25–27].

The morphology of $CdMoO_4$-SE was studied by FESEM, as shown in Fig. 2(a). It can be observed that most of micro-sized particles are connected with each other and still forms holes of different sizes. Such porous channel contributes to diffusion of the gas molecular within the material. Furthermore, EDS measurement was used to analysize the chemical composition and purity of $CdMoO_4$ sensing electrode material. As shown in Fig. 2(b), the obtained product consists of Cd, Mo and O elements, which means the sensing electrode material is free of impurity. For the single phase $CdMoO_4$, the elemental mapping measurement further confirms the coexistence and homogeneous dispersion of Cd, Mo and O elements.

To further illustrate the surface compositions and chemical states of the synthesized $CdMoO_4$ sensing electrode material, XPS analysis was investigated. The survey spectrum (Fig. 3a) demonstrates the prepared sensing material contains Cd, Mo, O and C elements. The carbon peak is assigned to the adventitious hydrocarbon from the XPS instrument itself [28]. The fitting peaks centered at 411.8 and 405 eV are assigned to Cd $3d_{3/2}$ and Cd $3d_{5/2}$, corresponding to $Cd^{2+}$ (Fig. 3b) [29,30]. As shown in Fig. 3c, two obvious peaks at 235.3 and 232.2 eV are ascribed to Mo $3d_{3/2}$ and Mo $3d_{5/2}$, respectively. The binding energy width of Mo 3d is equal to 3.1 eV, which can be confirmed Mo $^{6+}$ valence state [31–33]. In Fig. 3d, the binding energy peak positions at 532.3 and 530.3 eV could be attributed to chemisorbed oxygen species and $O^{2-}$ anions in the surface of $CdMoO_4$ material, respectively [34].

In order to appraise the effect of different sensing electrode materials on the sensing performances, the sensors attached with three different sensing electrodes ($CdMoO_4$, $CoMoO_4$ and $NiMoO_4$) were fabricated and the response values to 100 ppm acetone were measured and shown in Fig. 4. It is apparent that the sensor utilizing

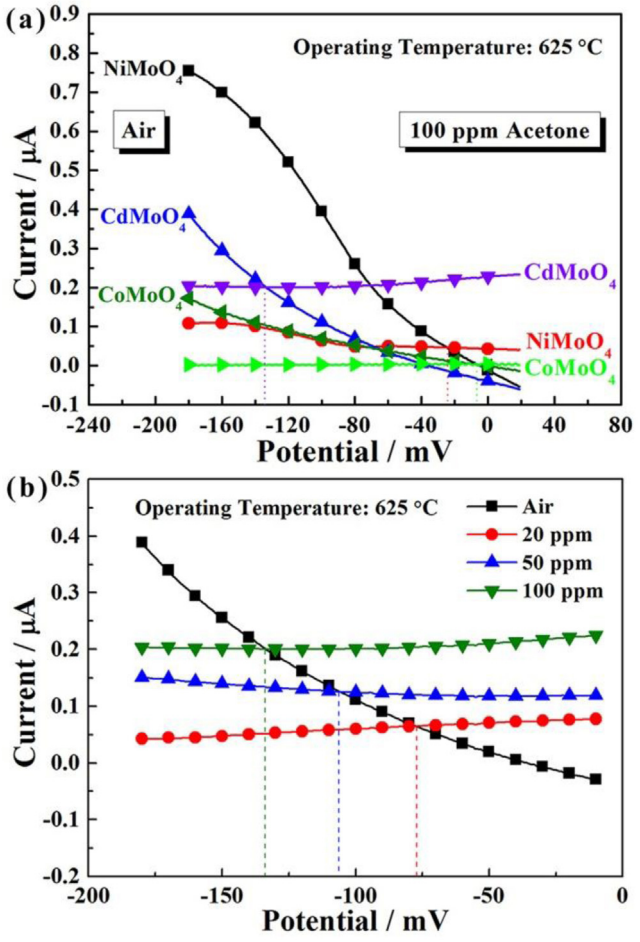


**Fig. 5.** (a) Polarization curves in air and 100 ppm acetone for the sensor using different sensing electrodes at 625 °C; (b) Polarization curves in different concentrations of acetone for the sensor attached with $CdMoO_4$-SE at 625 °C.

$CdMoO_4$-SE exhibited the almost highest response value to examined concentration of acetone comparing with the devices attached with other kinds of sensing electrodes. Therefore, the sensor using $CdMoO_4$-SE was paid considerable attentions to investigation in the following sections. The reason for this result may be partially explained from the following aspects. The sensing characteristics of the present devices abide by the mixed-potential theory, which has been demonstrated by Miura and co-workers [35–37]. Based on this, the sensor can be presented as the following electrochemical cells:

$$\text{Inair}: O_2, CdMoO_4/YSZ/Pt, O_2$$

$$\text{Insamplegas}: C_3H_6O + O_2, CdMoO_4/YSZ/Pt, C_3H_6O + O_2$$

Under the acetone gas atmosphere, the electrochemical reactions of cathodic (1) and anodic (2) (the cathodic reaction of $O_2$ and the anodic reaction of acetone) occur simultaneously at the TPB (triple phase boundary, the interface of $CdMoO_4$-SE, acetone and YSZ) and form a local cell. When the rates of two electrochemical reactions are equal to each other, the steady state condition is reached, and the electrode potential is called the mixed potential. The potential difference of the sensing electrode and reference electrode is obtained as the sensing signal.

$$\text{Cathodicreaction}: O_2 + 4e^- \rightarrow 2O^{2-} \quad (1)$$

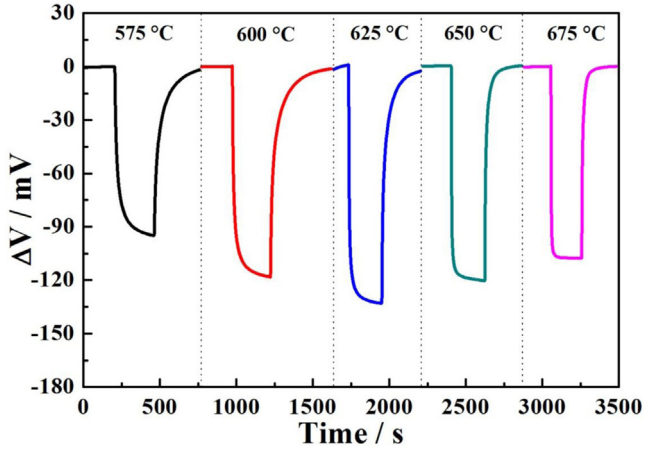


**Fig. 6.** Response and recovery transients for the sensor using $CdMoO_4$-SE to 100 ppm acetone at different operating temperatures.

$$\text{Anodicreaction}: 1/4C_3H_6O + 2O^{2-} \rightarrow 3/4CO_2 + 3/4H_2O + 4e^- \quad (2)$$

In regard to the present device, the mixed potential is strongly dependent on rates of electrochemical reactions (1) and (2) at TPB. In order to further illuminate the reason for the highest sensitivity of the sensor utilizing $CdMoO_4$-SE and validate the proposed mixed-potential mechanism, the polarization curves of the sensor attached with different sensing electrodes in air and 100 ppm acetone and the polarization curves of the sensor utilizing $CdMoO_4$-SE in different concentrations of acetone at 625 °C were measured and shown in Fig. 5. The cathodic polarization curve was obtained in air, and the anodic polarization curve was obtained by subtracting in air from in sample gas (different concentration of acetone + air). From the perspective of a mixed-potential model [36,38], good mixed potential response to acetone can be achieved by one or the combination of the following conditions: an increase in the anodic electrochemical reaction (2) and a decrease in the cathodic electrochemical reaction (1). It is obvious that the polarization curve for the anodic reaction of acetone for the device using $CdMoO_4$-SE shifts to higher current values, compared with others of those sensing electrodes. This indicates that sensor using $CdMoO_4$-SE exhibits the highest electrochemical catalytic activity to anodic reaction (2) of acetone. In this case, the sensor attached with $CdMoO_4$-SE displayed the highest response value to acetone at 625 °C. Additionally, the mixed potential can be estimated from the intersection of the cathodic and anodic polarization curves. By comparing the mixed potential estimated values and the potential difference values experimentally observed for fabricated sensors to different concentrations of acetone at 625 °C, in Table 1. The estimated values are in close proximity to those observed values under all circumstances. These coincidences further indicate that the present sensors supported the mixed potential sensing mechanism [39–41].

The response of the sensor is largely influenced by the operating temperature. Therefore, the responses of the sensor attached with $CdMoO_4$-SE towards 100 ppm acetone were investigated as a function of operating temperature. As indicated in Fig. 6, the response of present sensor to 100 ppm acetone displays a trend of "increase-maximum-decrease" and reaches a maximum value at 625 °C. At low operating temperature, the activation energy for electrochemical reaction is too deficient to achieve a relatively high response value. With increasing the working temperature, the electrochem-

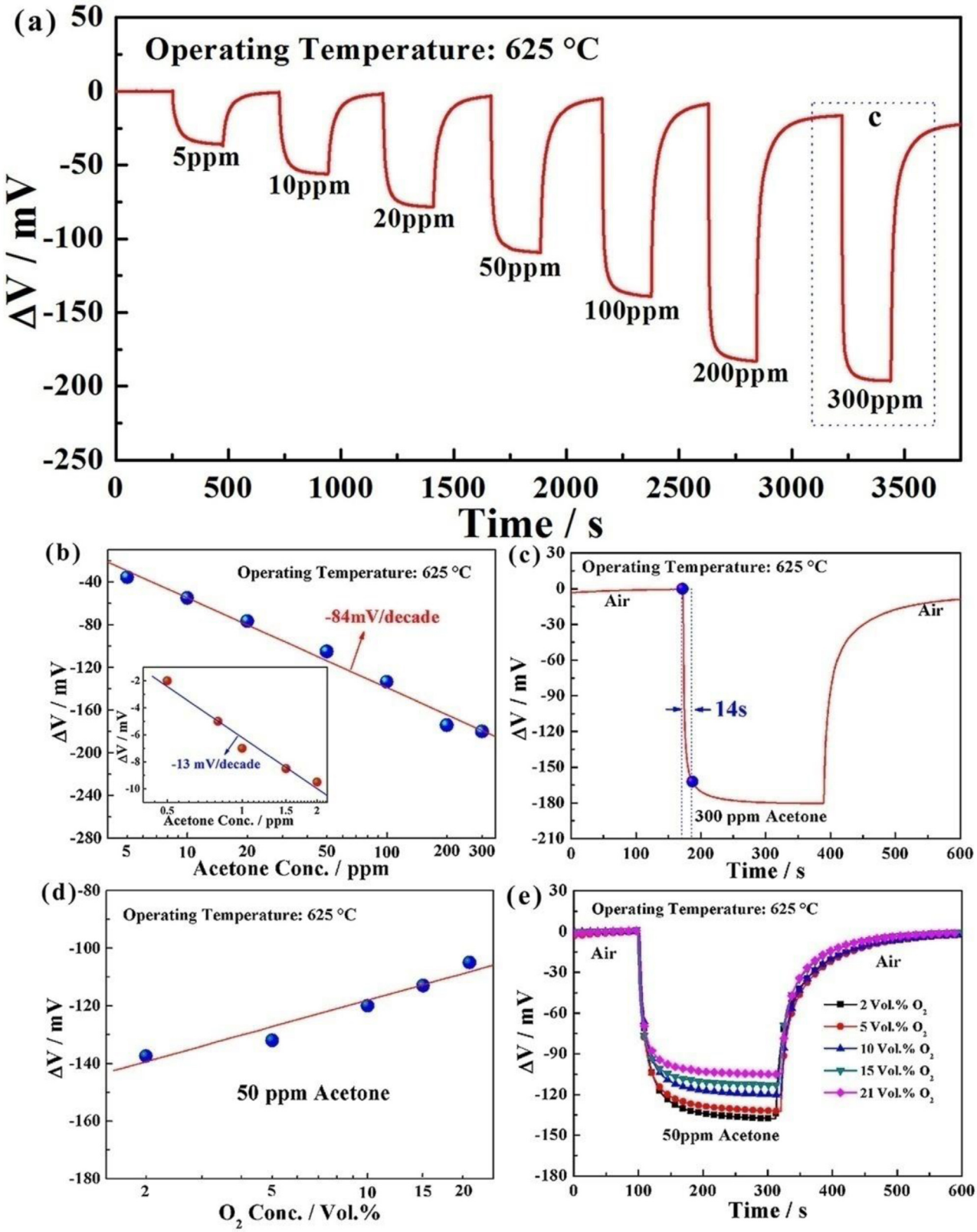


**Fig. 7.** (a) Response transients curve for the sensor attached with $CdMoO_4$-SE toward different concentrations of acetone in the range of 5–300 ppm at 625 °C; (b) Dependence of $\Delta V$ for the sensor attached with $CdMoO_4$-SE on the acetone concentration at 625 °C; (c) response and recovery times of present sensor to 300 ppm acetone; (d) Dependence of $\Delta V$ for the sensor to 50 ppm acetone on the logarithm of $O_2$ concentrations; (e) Response and recovery curves of the present sensor to 50 ppm acetone at different concentrations of $O_2$ at 625 °C.

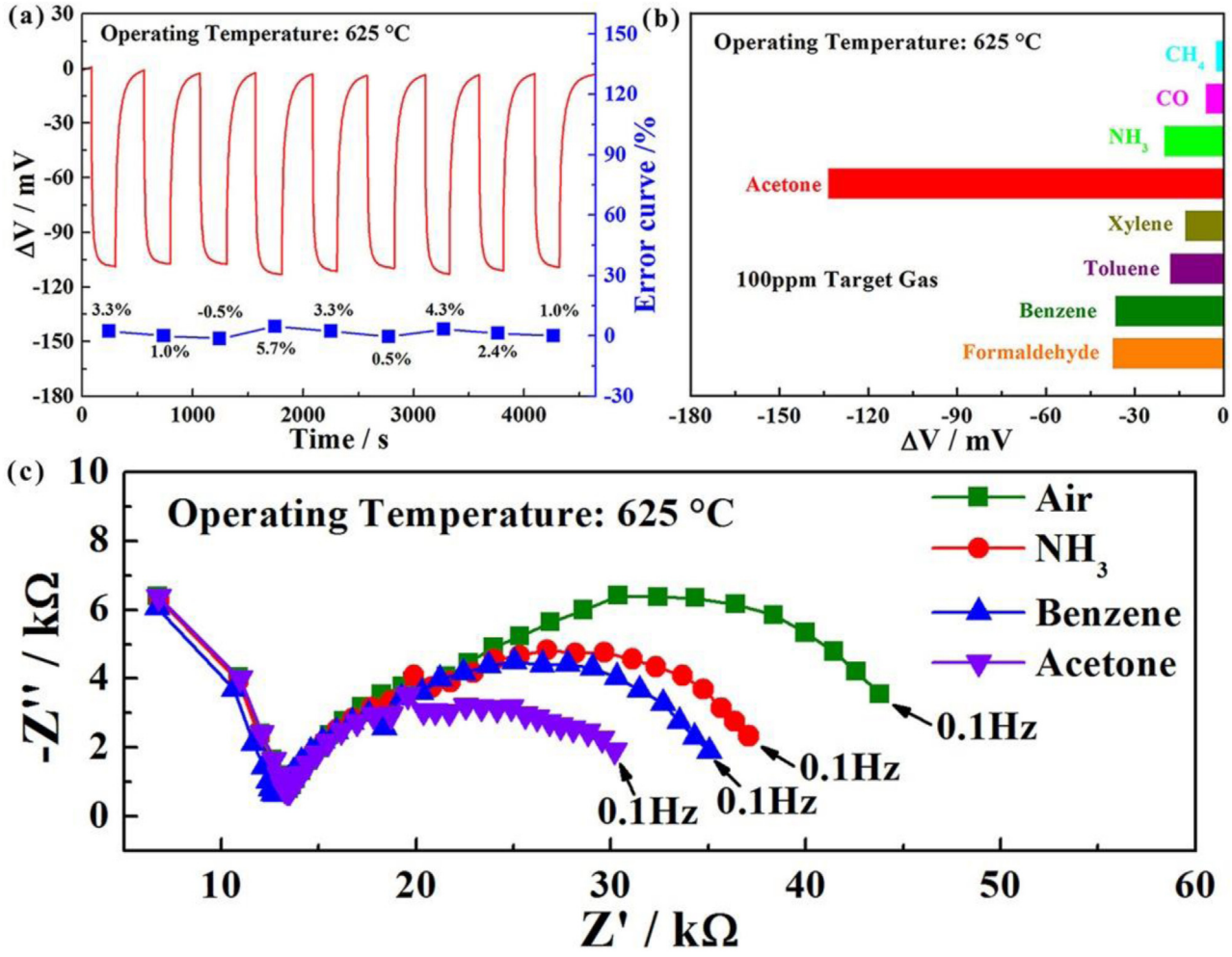


**Fig. 8.** (a) Continuous response-recovery transients to 50 ppm acetone for the sensor attached with $CdMoO_4$-SE at 625 °C; (b) Cross-sensitivities for the sensor attached with $CdMoO_4$-SE to 100 ppm of various deleterious gases at 625 °C; (c) Complex impedance curves of the present sensor in 100 ppm of various tested gases at 625 °C.

ical reaction at TPB will quickly accelerate, leading to improved response. While further increasing the operating temperature, the desorption process of acetone proceeds dominant, and the amount of acetone arrived at TPB decreases, which lead to deterioration of response at higher temperature. Consequently, the optimal operating temperature for the present sensor was considered to be 625 °C and was applied in measurement of sensing characteristics hereinafter.

The response transients of fabricated sensor attached with $CdMoO_4$-SE toward different concentrations of acetone in the range of 5–300 ppm was examined at 625 °C and the results obtained are shown in Fig. 7(a). The response of the sensor attached with $CdMoO_4$-SE to 100 ppm acetone at 625 °C was −133.5 mV. Furthermore, the dependence of ΔV for the sensor attached with $CdMoO_4$-SE on the acetone concentration in the examined range at 625 °C is shown in Fig. 7(b). In this regard, almost linear relationship between the ΔV and the logarithm of acetone concentration in the range of 5–300 ppm at 625 °C was observed, which abides by mixed potential type model. The sensitivity of the sensor using $CdMoO_4$-SE to acetone in the present concentration range was −84 mV/decade. Based on above results, the comparison of the acetone sensing property for the fabricated sensor and those reported previously in literature is presented in Table 2. Obviously, the present device exhibited better sensitivity to acetone than previously reported devices. Furthermore, it also can be seen from inset of Fig. 7(b) that the present sensor even could detect 500 ppb acetone, which the response value is −2 mV. The dependence of ΔV and logarithm of $NO_2$ concentration in the range of 0.5–2 ppm also displayed a linear relationship and the slope was −13 mV/decade. As shown in Fig. 7(c), the response time of the sensor to 300 ppm acetone at 625 °C are evaluated. It is seen that the 90% response time to 100 ppm acetone was 14 s, which exhibited improvable response rate comparing with the criterion of response time for mixed potential gas sensor reported by Zosel et al. [44]. Additionally, the effect of different oxygen concentration on acetone sensing performance is investigated at 625 °C. The dependence of ΔV for the sensor utilizing $CdMoO_4$-SE to 50 ppm acetone on the logarithm of $O_2$ concentrations at 625 °C was shown in Fig. 7(d). It can be seen that ΔV was almost positive linear to the logarithm of $O_2$ concentrations in the range of 2–21 Vol.% and the change of response value in the examined concentration range was 31%. Such result further demonstrated that the present sensor conformed to the mixed potential mechanism [36,45].

The continuous response and recovery and selectivity for gas sensor are important sensing performance parameters. The continuous response and recovery transients of the sensor utilizing $CdMoO_4$-SE to 50 ppm acetone at 625 °C, as illustrated in Fig. 8(a). It is clearly seen that the responses of the present device to 50 ppm acetone have little fluctuation and the best change error of continuous responses was 5.7% in the examined nine-time cycles, which indicates that the sensor exhibited good repeatability. Fig. 8(b) shows the cross-sensitivities for the sensor attached with $CdMoO_4$-

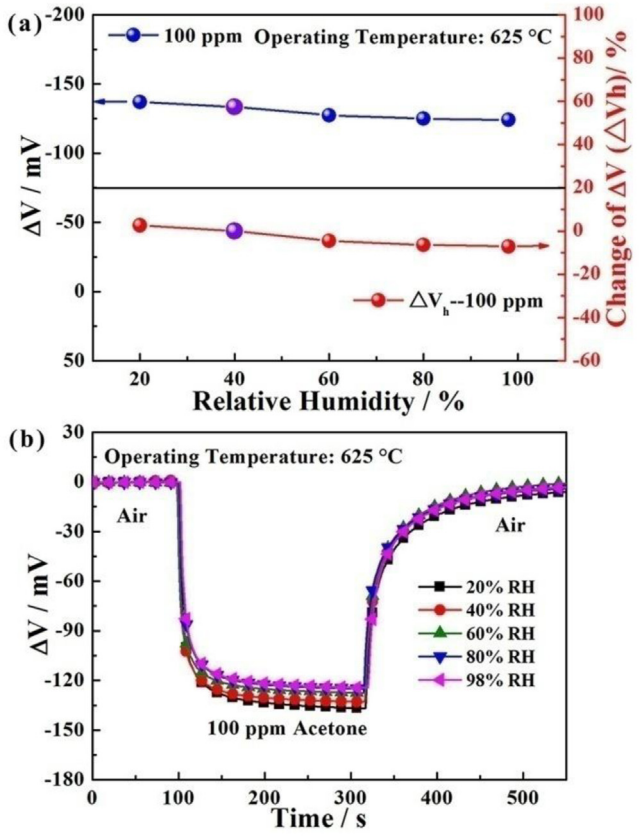


**Fig. 9.** (a) Response of the sensor attached with $CdMoO_4$-SE to 100 ppm acetone at 625 °C under different relative humidity; (b) Response and recovery transients for the sensor using $CdMoO_4$-SE to 100 ppm acetone under different relative humidity at 625 °C.

SE to various deleterious gases at 625 °C, such as formaldehyde, toluene, benzene and $NH_3$, etc. It is obvious that the present sensor exhibited the highest response values to 100 ppm acetone, and less effective response to any other tested gases. Therefore, the sensor using $CdMoO_4$-SE also showed good selectivity to acetone at 625 °C. Herein, in order to better understand the reason of good selectivity to acetone, the complex impedance of the present device in air and 100 ppm of various deleterious gases, such as acetone, toluene and $NH_3$ at 625 °C is measured and corresponding results are exhibited in Fig. 8(c). The resistance at higher frequencies for the sensor utilizing $CdMoO_4$-SE is mainly attributed to sensing electrode bulk resistance (including the small YSZ-bulk resistance). And the interfacial resistance is given by the resistance value at the intersection of the large semi-arc with the real axis at lower frequencies (around 0.1 Hz). Changes in the interface resistance measured in different atmosphere revealed the electrochemical catalytic activity toward the examined gas species [46]. Obviously, the resistance at high frequencies was almost constant in various measured gases, but the interfacial resistance in 100 ppm acetone was significantly decreased comparing with those of in other tested gases, which speculates the largest electrochemical catalytic reaction activity to acetone. Accordingly, the sensor attached with $CdMoO_4$-SE generated highest sensing magnitude toward acetone at 625 °C.

In addition, for a point of view in practical application of the sensor, the sensitivity to target gas should not be affected by the change in a surrounding condition and long-term use. The moisture resistance and stability of sensor are two vital factors for evaluating sensing performance, thus, the responses for the sensor attached with $CdMoO_4$-SE to 100 ppm acetone in the relative humidity (RH) range of 20–98% and the long-term stability of the present sensor

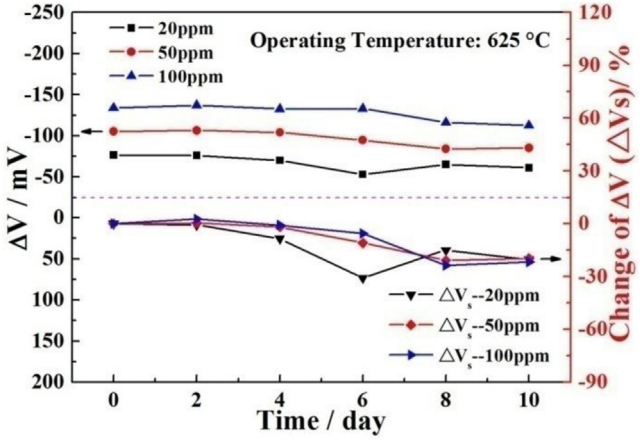


**Fig. 10.** Long-term stability to 20, 50 and 100 ppm acetone for the sensor attached with $CdMoO_4$-SE at 625 °C.

to 20, 50 and 100 ppm acetone at 625 °C are measured and results obtained are shown in Figs. 9 and 10. It can be seen that, in Fig. 9(a), the response value of the present sensor to 100 ppm acetone in the examined RH range displayed a relatively small change. In order to further illuminate quantitatively the change amplitude of the ΔV with relative humidity, the change of the ΔV ($\triangle V_h$) for the sensor is expressed by $\triangle V_h = [(\Delta V_n - \Delta V_0)/\Delta V_0 \times 100\%]$, where $\Delta V_n$ and $\Delta V_0$ denote the ΔV of the sensor under n% and 40% relative humidity, respectively. The result indicates that the response for fabricated sensor to 100 ppm acetone exhibits the change amplitude of −7.1%–2.6%, which demonstrates little effect on the sensing performance of the sensor. Furthermore, the stability of the sensor present fabricated was investigated by continuous working at high temperature of 625 °C during interval of 10 days. The responses of the sensor to 20, 50 and 100 ppm acetone were measured every other day. From Fig. 10, it can be also seen that the change amplitude of the ΔV for the sensor attached with $CdMoO_4$-SE changed slightly to 20, 50 and 100 ppm acetone during 10 days measurement period. The quantitative results showed that $\triangle V_s$ for the sensor to 20, 50 and 100 ppm acetone on the 10th day were −20.3%, −19.8% and −21.7%, respectively. Therefore, the present fabricated sensors showed the excellent moisture resistance and the acceptable stability during the measurement period.

## 4. Conclusion

In summary, $CdMoO_4$ as a new sensing electrode material was developed and for the first time applied in fabrication of highly sensitive mixed potential type YSZ-based gas sensors for detection of acetone at 625 °C. The responses of the sensors using different sensing electrodes ($CdMoO_4$, $CoMoO_4$ and $NiMoO_4$) were investigated and the result indicated that the sensor attached with $CdMoO_4$-SE displayed the highest response value to 100 ppm acetone at 625 °C. Additionally, the present sensor showed the low detection limit, high sensitivity, good selectivity to certain deleterious gases, the excellent moisture resistance and acceptable stability at 625 °C. For above-mentioned excellent sensing performance, the sensor developed has a good potential application prospect in acetone detection.

## Acknowledgements

This work is supported by the National Nature Science Foundation of China (Nos. 61473132, 61327804, 61374218, 61533021, 61520106003 and 61474057), Program for Chang Jiang Scholars and Innovative Research Team in University (No. IRT13018) and

National High-Tech Research and Development Program of China (863 Program, No. 2014AA06A505), Science and Technology Development Plan of Jilin Province (20140622005JC), Project 2016028 Supported by Graduate Innovation Fund of Jilin University.

## References


[1] S. Wang, J. Hao, Air quality management in China: issues, challenges, and options, J. Environ. Sci. 24 (2012) 2–13.
[2] E. Schneidemesser, P. Monks, C. Plass-Duelmer, Global comparison of VOC and CO observations in urban areas, Atmos. Environ. 44 (2010) 5053–5064.
[3] H. Guo, H. Cheng, Z. Ling, P. Louie, G. Ayoko, Which emission sources are responsible for the volatile organic compounds in the atmosphere of Pearl River Delta? J. Hazard. Mater. 188 (2011) 116–124.
[4] J. Tsai, P. Huang, H. Chiang, Characteristics of volatile organic compounds from motorcycle exhaust emission during real-world driving, Atmos. Environ. 99 (2014) 215–226.
[5] H. Guo, Z. Ling, H. Cheng, I. Simpson, X. Lyu, X. Wang, M. Shao, H. Lu, G. Ayoko, Y. Zhang, S. Saunders, S. Lam, J. Wang, D. Blake, Tropospheric volatile organic compounds in China, Sci. Total Environ. 574 (2017) 1021–1043.
[6] C. Deng, J. Zhang, X. Yu, W. Zhang, X. Zhang, Determination of acetone in human breath by gas chromatography-mass spectrometry and solid-phase microextraction with on-fiber derivatization, J. Chromatogr. B. 810 (2004) 269–275.
[7] M. Shnayderman, B. Mansfield, P. Yip, H. Clark, M. Krebs, S. Cohen, J. Zeskind, E. Ryan, H. Dorkin, M. Callahan, T. Stair, J. Gelfand, C. Gill, B. Hitt, C. Davis, Species-specific bacteria identification using differential mobility spectrometry and bioinformatics pattern recognition, Anal. Chem. 77 (2005) 5930–5937.
[8] S. Choi, W. Ryu, S. Kim, H. Cho, I. Kim, Bi-functional co-sensitization of graphene oxide sheets and Ir nanoparticles on p-type $Co_3O_4$ nanofibers for selective acetone detection, J. Mater. Chem. B 2 (2014) 7160–7167.
[9] N. Miura, S. Zhuiykov, T. Ono, M. Hasei, N. Yamazoe, Mixed potential type sensor using stabilized zirconia and $ZnFe_2O_4$ sensing electrode for $NO_x$ detection at high temperature, Sens. Actuators B: Chem. 83 (2002) 222–229.
[10] H. Giang, H. Duy, P. Ngan, G. Thai, D. Thu, N. Toan, High sensitivity and selectivity of mixed potential sensor based on Pt/YSZ/$SmFeO_3$ to $NO_2$ gas, Sens. Actuators B: Chem. 183 (2013) 550–555.
[11] Q. Diao, C. Yin, Y. Liu, J. Li, X. Gong, X. Liang, S. Yang, H. Chen, G. Lu, Mixed-potential-type $NO_2$ sensor using stabilized zirconia and $Cr_2O_3$-$WO_3$ nanocomposites, Sens. Actuators B: Chem. 180 (2013) 90–95.
[12] P. Elumalai, V. Plashnitsa, Y. Fujio, N. Miura, Stabilized zirconia-based sensor attached with NiO/Au sensing electrode aiming for highly selective detection of ammonia in automobile exhausts, Electrochem. Solid-State Lett. 11 (2008) J79–J81.
[13] I. Lee, B. Jung, J. Park, C. Lee, J. Hwang, C. Park, Mixed potential $NH_3$ sensor with $LaCoO_3$ reference electrode, Sens. Actuators B: Chem. 176 (2013) 966–970.
[14] F. Liu, R. Sun, Y. Guan, X. Cheng, H. Zhang, Y. Guan, X. Liang, P. Sun, G. Lu, Mixed-potential type $NH_3$ sensor based on stabilized zirconia and $Ni_3V_2O_8$ sensing electrode, Sens. Actuators B: Chem. 210 (2015) 795–802.
[15] N. Miura, T. Raisen, G. Lu, N. Yamazoe, Highly selective CO sensor using stabilized zirconia and a couple of oxide electrodes, Sens. Actuators B: Chem. 47 (1998) 84–91.
[16] Y. Fujio, V. Plashnitsa, M. Breedon, N. Miura, Construction of sensitive and selective zirconia-based CO sensors using $ZnCr_2O_4$-based sensing electrodes, Langmuir 28 (2012) 1638–1645.
[17] Y. Guan, C. Yin, X. Cheng, X. Liang, Q. Diao, H. Zhang, G. Lu, Sub-ppm $H_2S$ sensor based on YSZ and hollow balls $NiMn_2O_4$ sensing electrode, Sens. Actuators B: Chem. 193 (2014) 501–508.
[18] T. Sato, V. Plashnitsa, M. Utiyama, N. Miura, Potentiometric YSZ-based sensor using NiO sensing electrode aiming at detection of volatile organic compounds (VOCs) in air environment, Electrochem. Commun. 12 (2010) 524–526.
[19] Y. Fujio, V. Plashnitsa, P. Elumalai, N. Miura, Stabilization of sensing performance for mixed-potential-type zirconia-based hydrocarbon sensor, Talanta 85 (2011) 575–581.
[20] Y. Suetsugu, T. Sato, M. Breedon, N. Miura, $C_3H_6$ sensing characteristics of rod-type yttria-stabilized zirconia-based sensor for ppb level environmental monitoring applications, Electrochim. Acta 73 (2012) 118–122.
[21] F. Liu, Y. Guan, R. Sun, X. Liang, P. Sun, F. Liu, G. Lu, Mixed potential type acetone sensor using stabilized zirconia and $M_3V_2O_8$ (M: Zn Co and Ni) sensing electrode, Sens. Actuators B: Chem. 221 (2015) 673–680.
[22] F. Liu, X. Yang, B. Wang, Y. Guan, X. Liang, P. Sun, G. Lu, High performance mixed potential type acetone sensor based on stabilized zirconia and $NiNb_2O_6$ sensing electrode, Sens. Actuators B: Chem. 229 (2016) 200–208.
[23] Q. Diao, C. Yin, Y. Guan, X. Liang, S. Wang, Y. Liu, Y. Hu, H. Chen, G. Lu, The effects of sintering temperature of $MnCr_2O_4$ nanocomposite on the $NO_2$ sensing property for YSZ-based potentiometric sensor, Sens. Actuators B: Chem. 177 (2013) 397–403.
[24] C. Wang, X. Cheng, X. Zhou, P. Sun, X. Hu, K. Shimanoe, G. Lu, N. Yamazoe, Hierarchical α-$Fe_2O_3$/NiO composites with a hollow structure for a gas sensor, ACS Appl. Mater. Interfaces 6 (2014) 12031–12037.
[25] Z. Shahri, A. Sobhani, M. Salavati-Niasari, Controllable synthesis and characterization of cadmium molybdate octahedral nanocrystals by coprecipi- tation method, Mater. Res. Bull. 48 (2013) 3901–3909.
[26] A. Phuruangrat, N. Ekthammathat, T. Thongtem, S. Thongtem, Microwave-assisted synthesis and optical property of $CdMoO_4$ nanoparticles, J. Phys. Chem. Solids 72 (2011) 176–180.
[27] S. Hosseinpour-Mashkani, M. Maddahfar, A. Sobhani-Nasab, Novel silver-doped $CdMoO_4$: synthesis, characterization, and its photocatalytic performance for methyl orange degradation through the sonochemical method, J. Mater. Sci. Mater. Electron. 27 (2016) 474–480.
[28] J. Moulder, W. Stickle, P. Sobol, K. Bomben, Handbook of X-ray Photoelectron Spectroscopy, 2nd ed., Perkin Elmer Corp., Eden Prairie, MN, USA, 1992.
[29] P. Madhusudan, J. Zhang, B. Cheng, J. Yu, Fabrication of $CdMoO_4$@CdS core-shell hollow superstructures as high performance visible-light driven photocatalysts, Phys. Chem. Chem. Phys. 17 (2015) 15339–15347.
[30] J. Bi, Z. Zhou, M. Chen, S. Liang, Y. He, Z. Zhang, L. Wu, Plasmonic Au/$CdMoO_4$ photocatalyst: influence of surface plasmon resonance for selective photocatalytic oxidation of benzylic alcohol, Appl. Surf. Sci. 349 (2015) 292–298.
[31] Z. Chen, D. Cummins, B. Reinecke, E. Clark, M. Sunkara, T. Jaramillo, Core-shell $MoO_3$-$MoS_2$ nanowires for hydrogen evolution: a functional design for electrocatalytic materials, Nano Lett. 11 (2011) 4168–4175.
[32] M. Yu, L. Jiang, H. Yang, Ultrathin nanosheets constructed $CoMoO_4$ porous flowers with high activity for electrocatalytic oxygen evolution, Chem. Commun. 51 (2015) 14361–14364.
[33] H. Liu, L. Tan, Synthesis, structure, and electrochemical properties of $CdMoO_4$ nanorods, Ionics 16 (2010) 57–60.
[34] P. Madhusudan, J. Zhang, J. Yu, B. Cheng, D. Xu, J. Zhang, One-pot template-free synthesis of porous $CdMoO_4$ microspheres and their enhanced photocatalytic activity, Appl. Surf. Sci. 387 (2016) 202–213.
[35] N. Miura, G. Lu, N. Yamazoe, Progress in mixed-potential type devices based on solid electrolyte for sensing redox gases, Solid State Ionics 136–137 (2000) 533–542.
[36] N. Miura, T. Sato, S. Anggraini, H. Ikeda, S. Zhuiykov, A review of mixed-potential type zirconia-based gas sensors, Ionics 20 (2014) 901–925.
[37] V. Plashnitsa, T. Ueda, N. Miura, Improvement of $NO_2$ a sensing performances by an additional second component to the nano-structured NiO sensing electrode of a YSZ-based mixed-potential type sensor, Int. J. Appl. Ceram. Technol. 3 (2006) 127–133.
[38] N. Szabo, P. Dutta, Correlation of sensing behavior of mixed potential sensors with chemical and electrochemical properties of electrodes, Solid State Ionics 171 (2004) 183–190.
[39] G. Lu, Q. Diao, C. Yin, S. Yang, Y. Guan, X. Cheng, X. Liang, High performance mixed-potential type $NO_x$ sensor based on stabilized zirconia and oxide electrode, Solid State Ionics 262 (2014) 292–297.
[40] P. Elumalai, J. Wang, S. Zhuiykov, D. Terada, M. Hasei, N. Miura, Sensing characteristics of YSZ-based mixed-potential-type planar $NO_x$ sensors using NiO sensing electrodes sintered at different temperatures, J. Electrochem. Soc. 152 (2005) H95–H101.
[41] T. Sato, V. Plashnitsa, M. Utiyama, N. Miura, Potentiometric YSZ-based sensor using NiO sensing electrode aiming at detection of volatile organic compounds (VOCs) in air environment, Electrochem. Commun. 12 (2010) 524–526.
[42] H. Zhang, C. Yin, Y. Guan, X. Cheng, X. Liang, G. Lu, NASICON-based acetone sensor using three-dimensional three-phase boundary and Cr-based spinel oxide sensing electrode, Solid State Ionics 262 (2014) 283–287.
[43] M. Kasalizadeh, A. Khodadadi, Y. Mortazavi, Coupled metal oxide-doped Pt/$SnO_2$ semiconductor and yittria-stabilized zirconia electrochemical sensors for detection of VOCs, J. Electrochem. Soc. 160 (2013) B218–B224.
[44] J. Zosel, D. Tuchtenhagen, K. Ahlborn, U. Guth, Mixed potential gas sensor with short response time, Sens. Actuators B: Chem. 130 (2008) 326–329.
[45] G. Lu, N. Miura, N. Yamazoe, High-temperature sensors for NO and $NO_2$ based on stabilized zirconia and spinel-type oxide electrode, J. Mater. Chem. 7 (1997) 1445–1449.
[46] N. Miura, M. Nakatou, S. Zhuiykov, Impedancemetric gas sensor based on zirconia solid electrolyte and oxide sensing electrode for detecting total $NO_x$ at high temperature, Sens. Actuators B: Chem. 93 (2003) 221–228.


## Biographies

**Fangmeng Liu** received his B.S. degree in 2009 from College of Chemistry, Liaocheng University and M.S. degree in 2012 from Northeast Forestry University in China. Currently he is studying for his Ph.D. degree in College of Electronic Science and Engineering, Jilin University, China.

**Ce Ma** received the B.Eng. degree in department of electronic science and technology in 2016. He is currently studying for his M.E. Sci. degree in College of Electronic Science and Engineering, Jilin University, China.

**Xidong Hao** received the B.Eng. degree in department of electronic science and technology in 2016. He is currently studying for his M.E. Sci. degree in College of Electronic Science and Engineering, Jilin University, China.

**Chunhua Yang** is a professor and works in School of Information Science and Engineering, Central South University, China. Her research interests are focused on automation and computer control.

**Hongqiu Zhu** is an associate professor and works in School of Information Science and Engineering, Central South University, China. His research interests are focused on automation and computer control.

**Xishuang Liang** received the B. Eng. degree in Department of Electronic Science and Technology in 2004. He received his Doctor's degree in College of Electronic Science and Engineering at Jilin University in 2009. Now he is an associate professor of Jilin University, China. His current research is solid electrolyte gas sensor.

**Peng Sun** received his PhD degree from the Electronics Science and Engineering department, Jilin University, China in 2014. Now, he is engaged in the synthesis and characterization of the semiconducting functional materials and gas sensors.

**Fengmin Liu** received the BE degree in Department of Electronic Science and Technology in 2000. She received his Doctor's degree in College of Electronic Science and Engineering at Jilin University in 2005. Now she is a professor in Jilin University, China. Her current research is preparation and application of semiconductor oxide, especial in gas sensor and solar cell.

**Xiaohong Chuai** is an associate professor and works in Department of Electrical Engineering, Jilin University, China. Her research interests are focused on sensor materials and devices.

**Geyu Lu** received the B.Sci. degree in electronic sciences in 1985 and the M.S. degree in 1988 from Jilin University in China and the Dr. Eng. degree in 1998 from Kyushu University in Japan. Now he is a professor of Jilin University, China. His current research interests include the development of chemical sensors and the application of the function materials.